

# VIBRATIONAL RELAXATION OF *NO* SCATTERING FROM *AU(111)*

---

VISTA Seminar

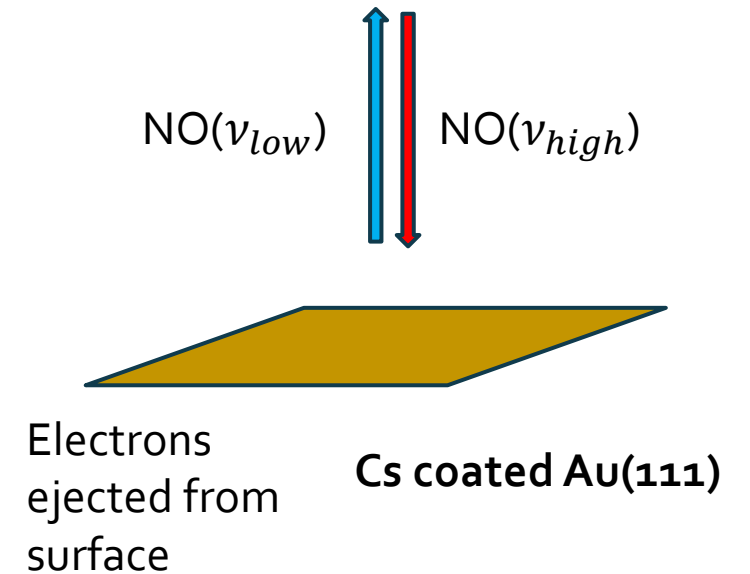
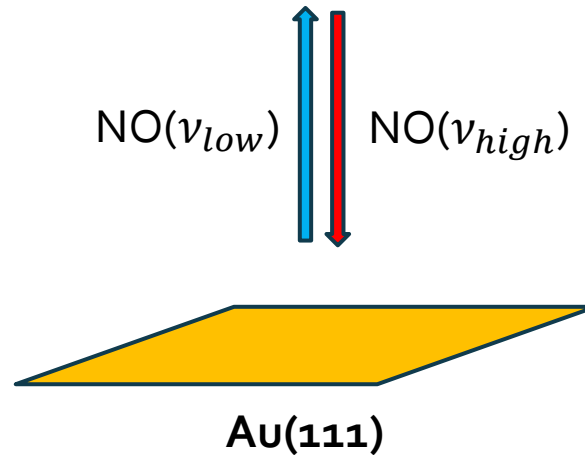
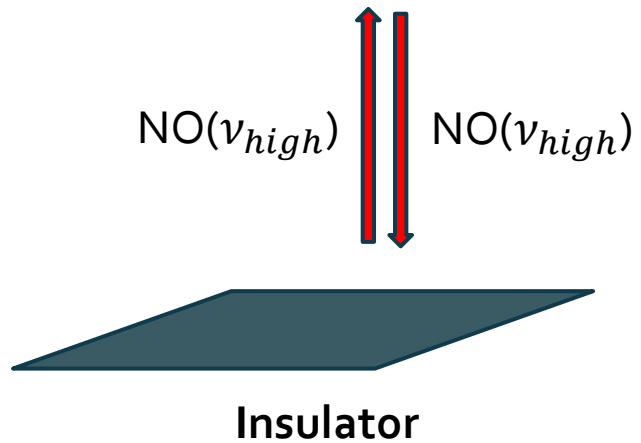
6<sup>th</sup> March 2024

Shreyas Malpathak

Ananth Group

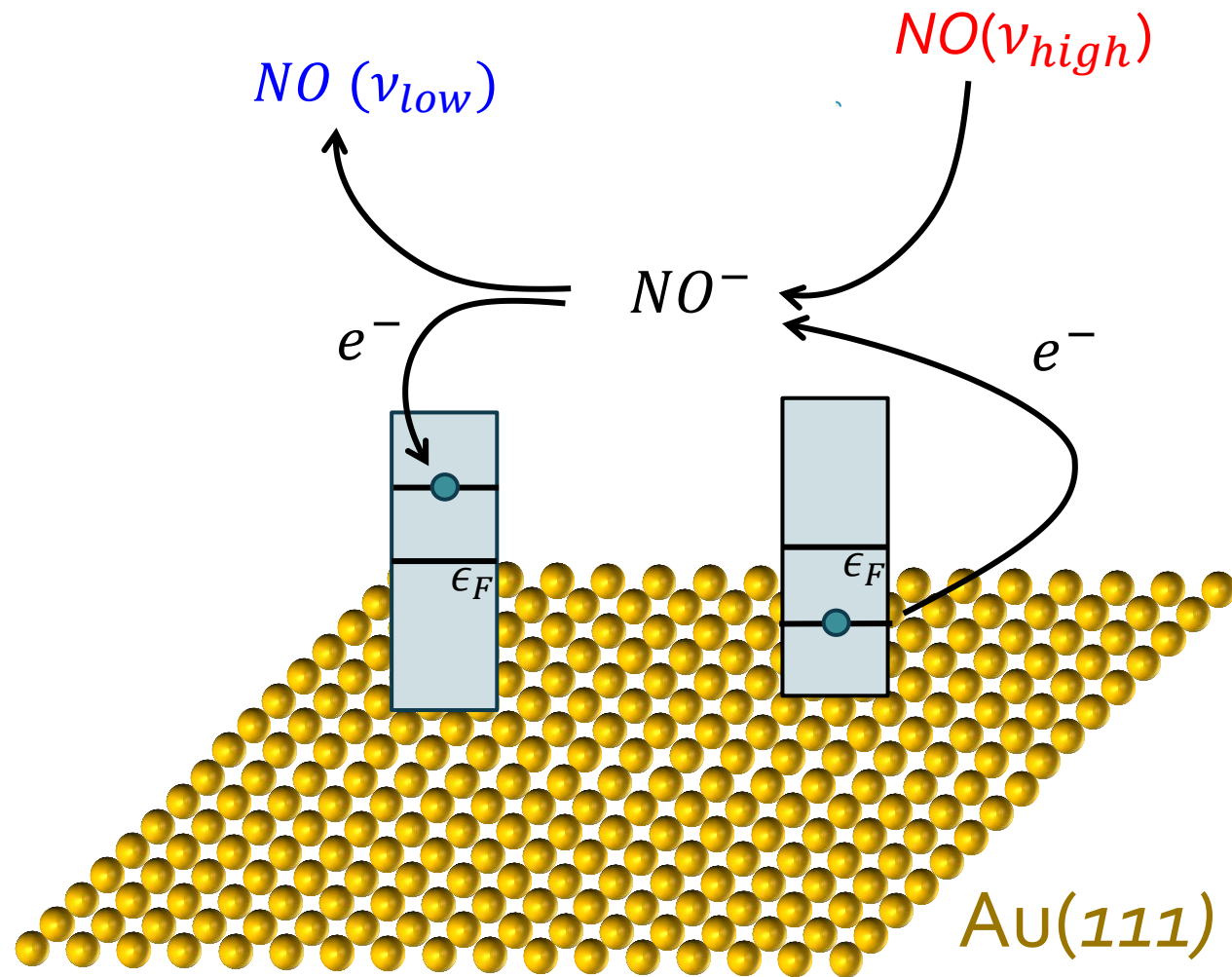
Cornell University

# NO scattering from Au(111)



# Proposed mechanism

*Vibrational energy  
is lost into  
electron hole pair  
excitations*



# Prominent simulation approaches

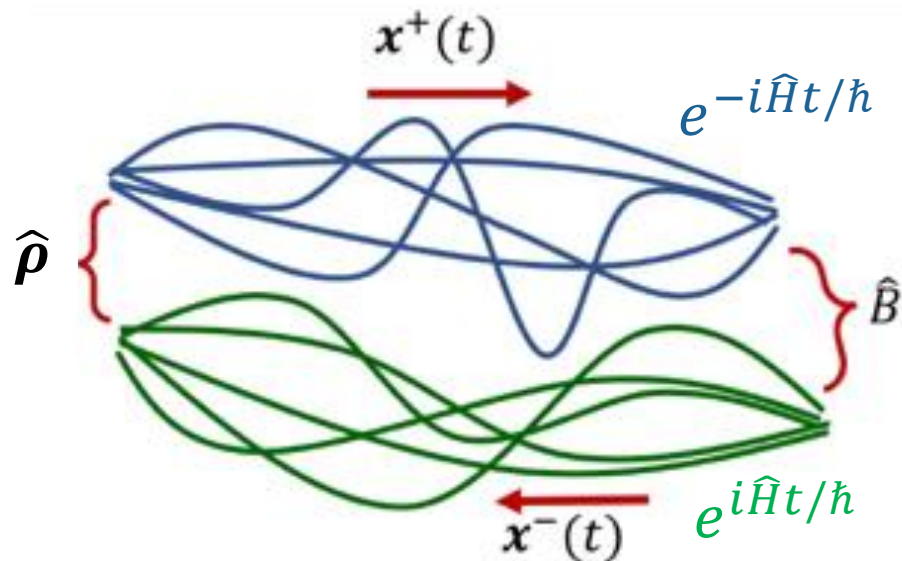
- Independent Electron Surface Hopping (IESH)<sup>[1]</sup>
- Molecular Dynamics with Electronic Friction (MDEF)<sup>[2]</sup>
- Semiclassical Dynamics?

- [1] Shenvi et.al. *J. Chem. Phys.*, 130,174107 (2009)

- [2] Head-Gordon & Tully, *J. Chem. Phys.*, 103, 10137 (1995)

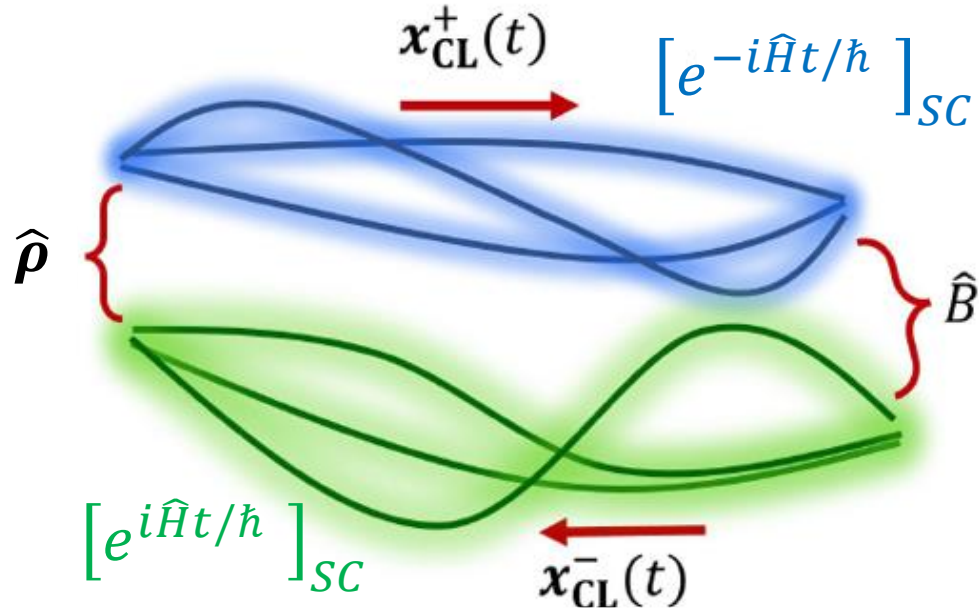
# Quantum dynamics with path integrals

$$\langle \hat{B}(t) \rangle = \text{Tr}[\hat{\rho} \hat{B}(t)] = \text{Tr}[\hat{\rho} e^{i\hat{H}t/\hbar} \hat{B} e^{-i\hat{H}t/\hbar}]$$



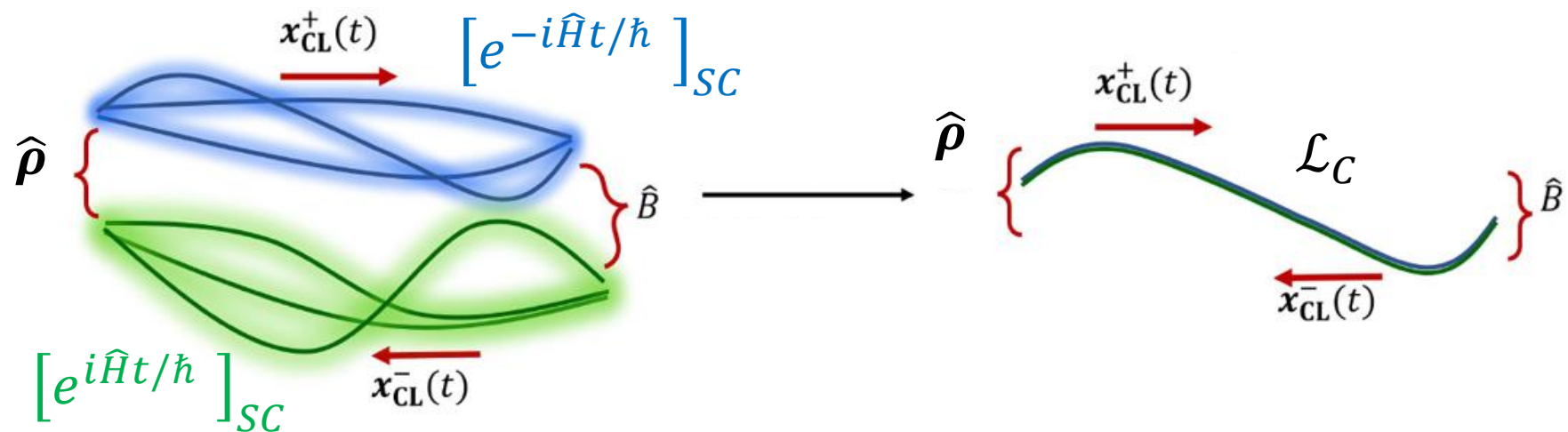
- Count **ALL** forward and backward paths
- Weight them by their action:  $e^{i(S^+ - S^-)/\hbar}$

# Semiclassical (SC) dynamics



- Use Stationary Phase Approximation (SPA) to path integral of propagator: Only count classical paths .
- SC pre-factor accounts for `quantum fluctuations around classical paths.
- Trajectories interfere with each other through their classical actions.
- Can account for most quantum effects: ZPE, shallow tunneling, interference.

# Classical-limit SC dynamics



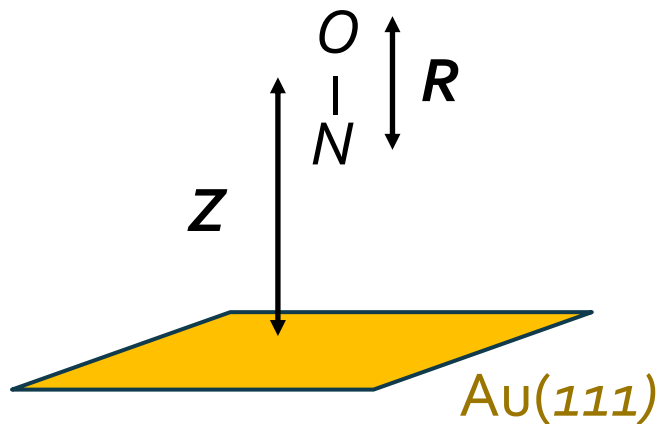
- Assume forward  $[x_{cl}^+(t)]$  and backward  $[x_{cl}^-(t)]$  trajectories coincide.
- Evolve ensemble of classical trajectories from a quantum distribution.

-Miller, *J. Phys. Chem. A*, **105**, 2942 (2001)

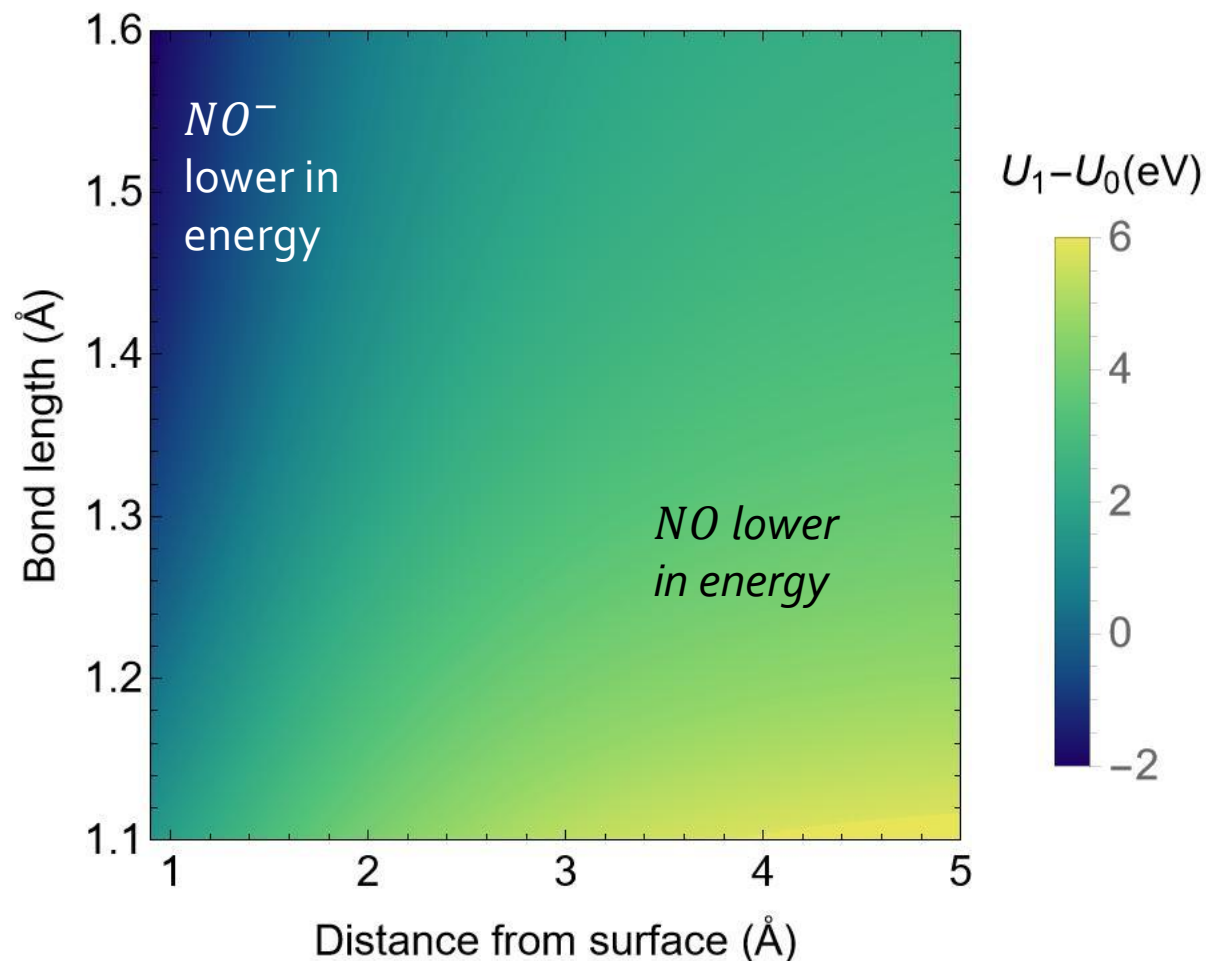
-Wang et. al., *J. Chem. Phys.*, 108, 9726 (1998), Sun et.al., *J. Chem. Phys.*, 109, 4190 (1998).

-Malpathak, Church, Ananth, *J. Phys. Chem. A* **126**, 6359 (2022)

# Some insights into the scattering process



*An elongated NO bond and proximity to the Au(111) surface facilitate electron transfer*





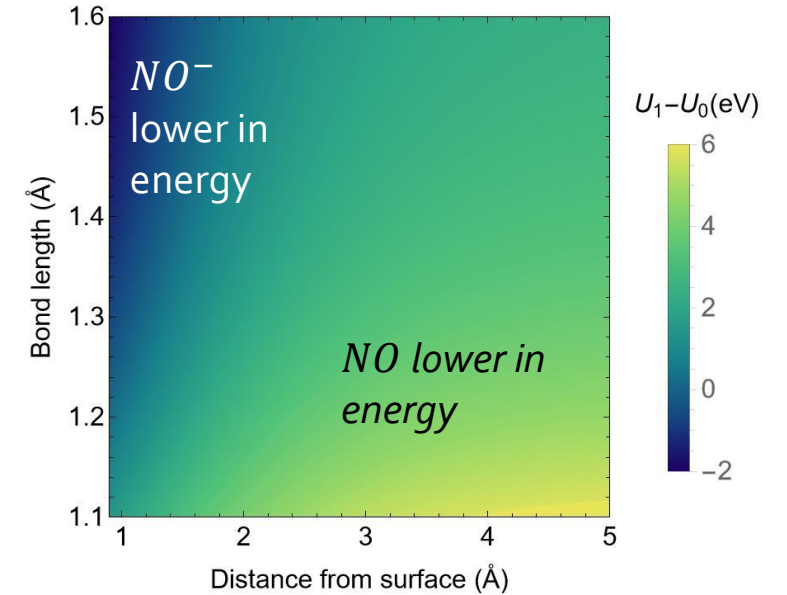
# Model Hamiltonian

## News-Anderson-Holstein Hamiltonian

$$H_{NAH}(\mathbf{X}, \mathbf{P}) = \frac{1}{2} \mathbf{P} \cdot \mathbf{m}^{-1} \cdot \mathbf{P} + U_0(\mathbf{X}) + [U_1(\mathbf{X}) - U_0(\mathbf{X})] d^\dagger d$$
$$+ \sum_k \epsilon_k c_k^\dagger c_k + \sum_k V_k(\mathbf{X}) (d^\dagger c_k + c_k^\dagger d)$$

Annotations:

- $NO$  potential (points to  $U_0(\mathbf{X})$ )
- $NO^-$  potential (points to  $[U_1(\mathbf{X}) - U_0(\mathbf{X})]$ )
- Metal states (points to  $\sum_k \epsilon_k c_k^\dagger c_k$ )
- Metal-molecule coupling (points to  $\sum_k V_k(\mathbf{X}) (d^\dagger c_k + c_k^\dagger d)$ )
- $NO^-$  occupation number (points to  $d^\dagger d$ )

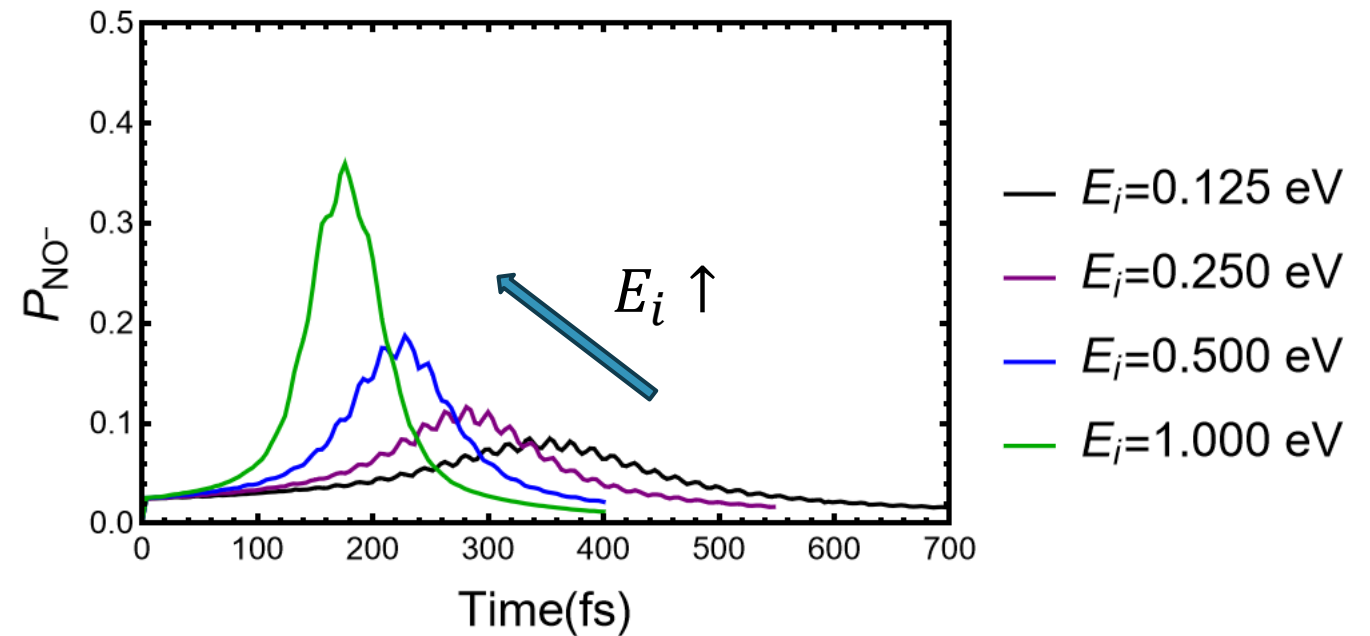
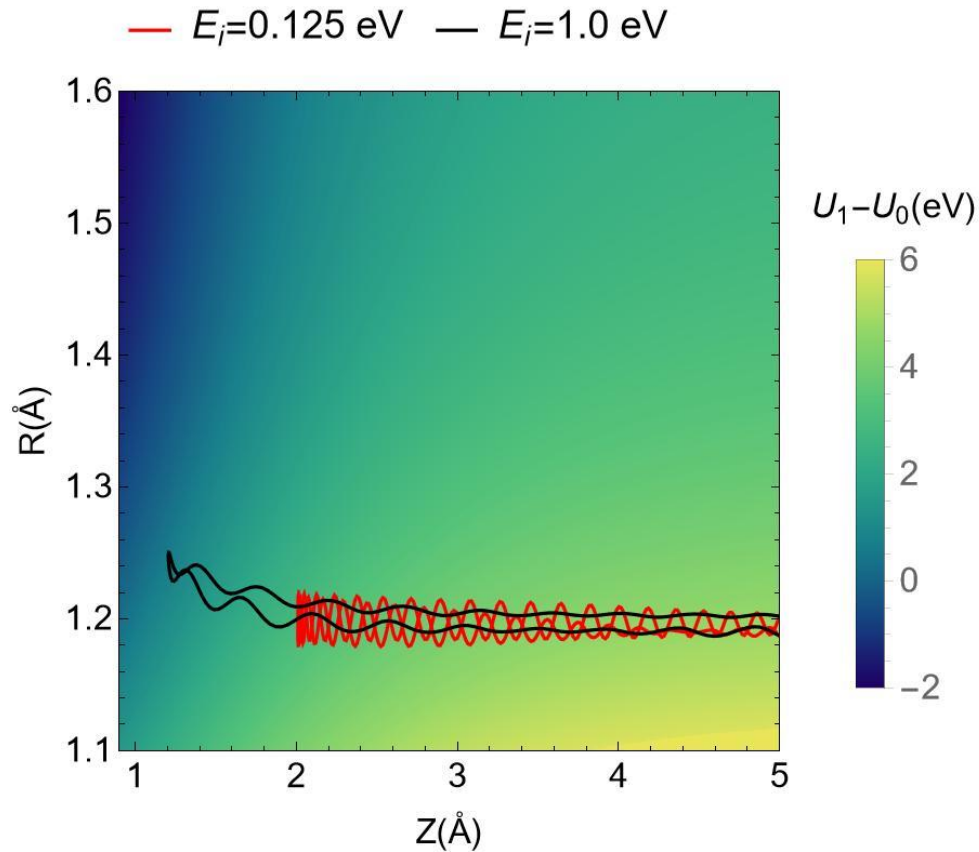


- Mapped onto continuous variables
- Use model parameters by Gardner et.al.

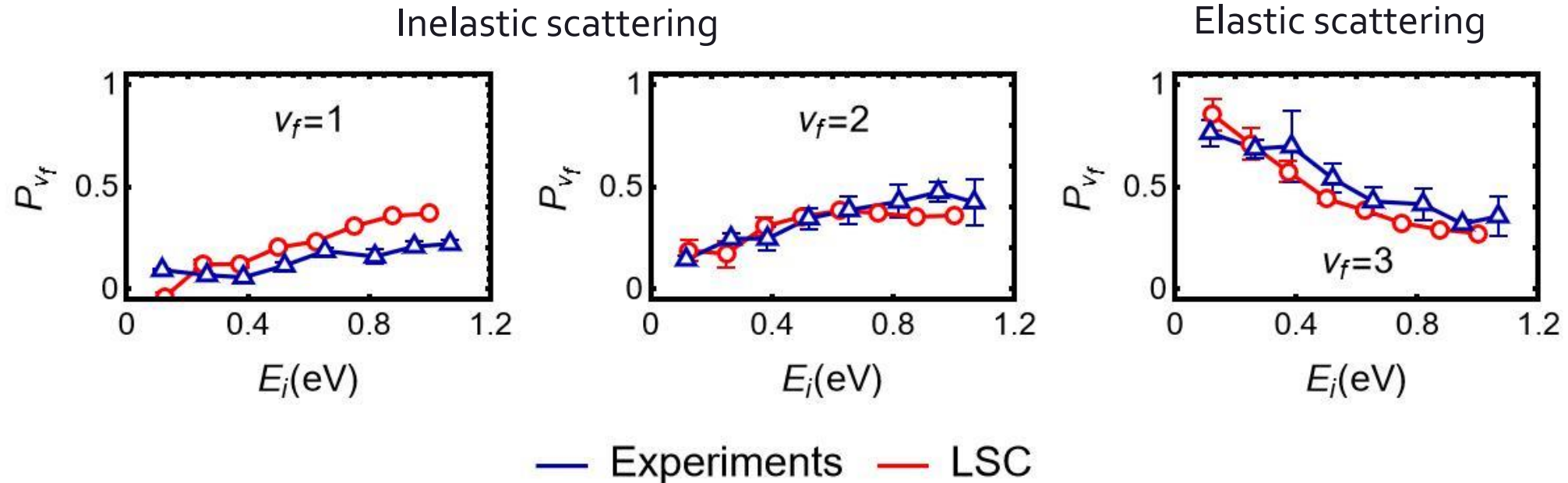
# $\nu_i = 3$ : shorter *NO* bond

For  $\nu_i = 3$ , as  $E_i \uparrow$ :

- *NO* approaches closer to surface
- Bond stretches more
- Extent of electron transfer  $\uparrow$

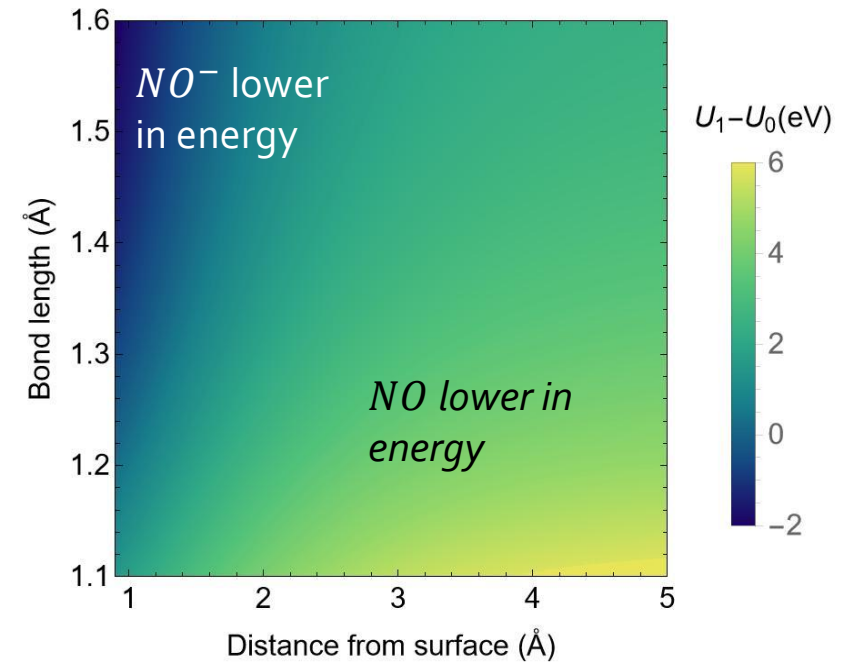
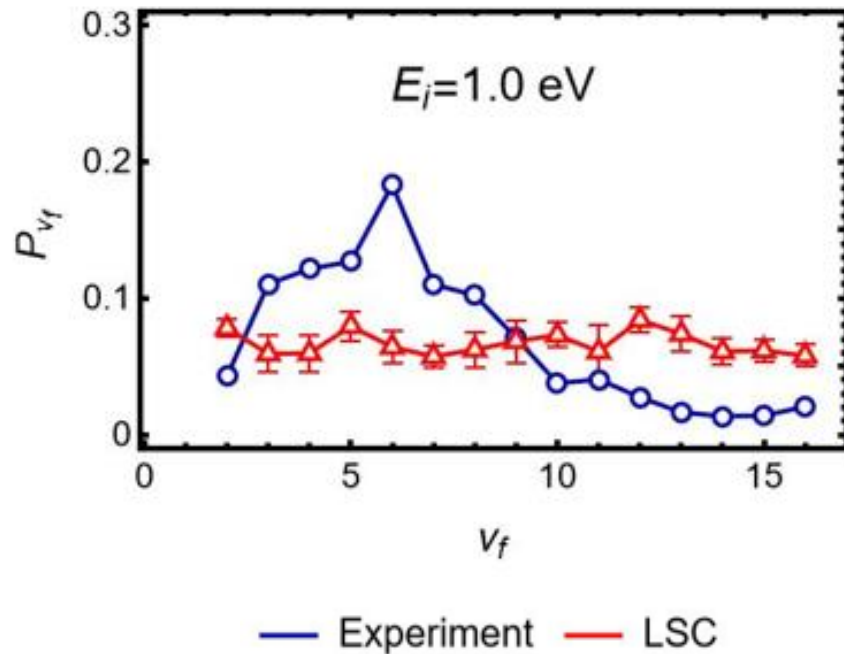


# Vibrational relaxation for $\nu_i = 3$



- Accurately captures role of transient electron transfer and incident translational energy
- Comparable to MDEF and IESH.

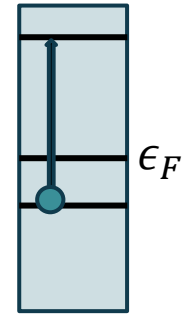
$\nu_i = 16$ : longer  $NO$  bond



*LSC is unable to predict experimental vibrational distributions.*

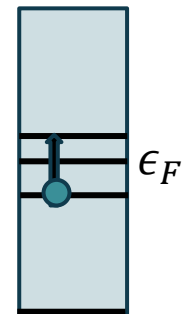
# Resonant vs. dissipative

Vibrational energy transferred into a few *high energy* EHP excitations

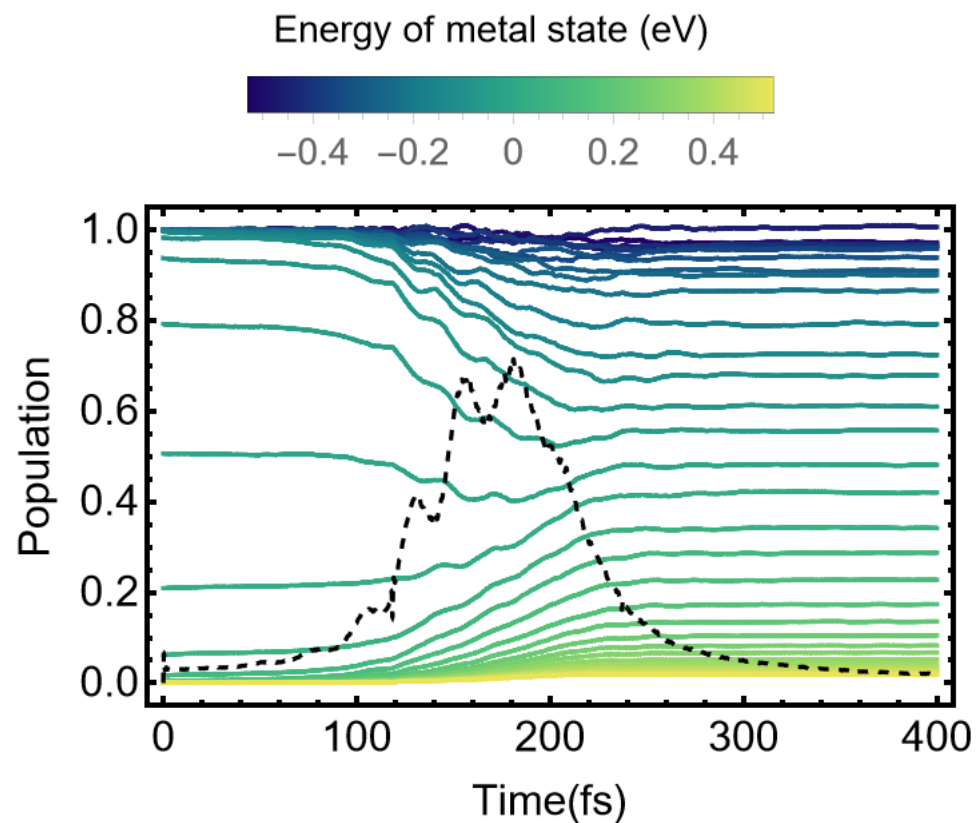
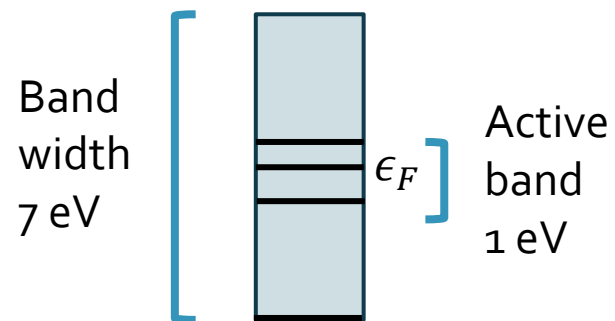


OR

Vibrational energy dissipated into many low energy EHP excitations



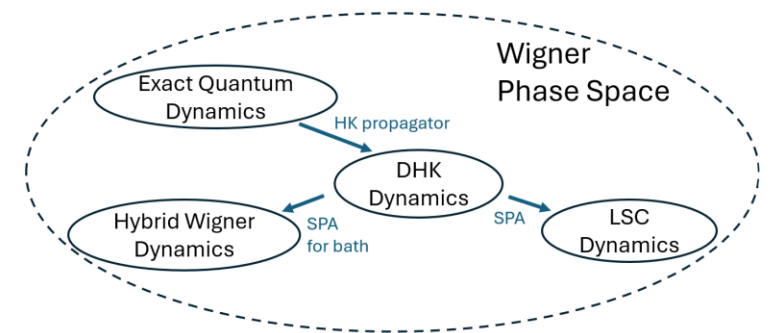
# Population of metal states



LSC is unable to capture a resonant mechanism for electron transfer

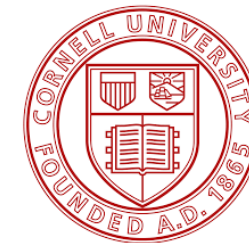
# Summary

- Can predict role of ET and dependence on translational energy in vibrational relaxation for short NO bond lengths.
- Like other state of the art methods, falls short for larger bond lengths. Unable to predict resonant ET mechanism.
- Need a better NAH model Hamiltonian that can account for orientation of NO, rotation and coupling to phonons.
- Quantizing NO vibration might provide a more accurate description of resonant ET. New method: **Hybrid Wigner Dynamics** is well suited for this.





# Thank you!



## Graduate Research Committee:

Prof. Nandini Ananth

Prof. Gregory Ezra

Prof. Roger Loring

Ananth Group Members

Cornell Dept. of Chemistry and  
NSF for funding





# Path integral for the propagator

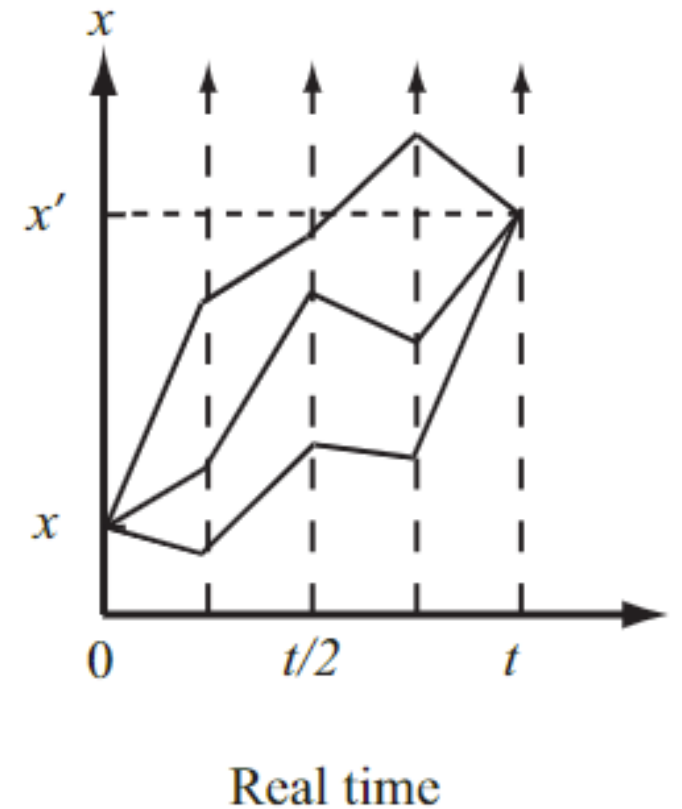
$$\langle x' | e^{-i\hat{H}t/\hbar} | x \rangle = \langle x' | e^{-i\hat{H}\epsilon/\hbar} e^{-i\hat{H}\epsilon/\hbar} \dots e^{-i\hat{H}\epsilon/\hbar} | x \rangle$$

$N$  of these,  $\epsilon = t/N$

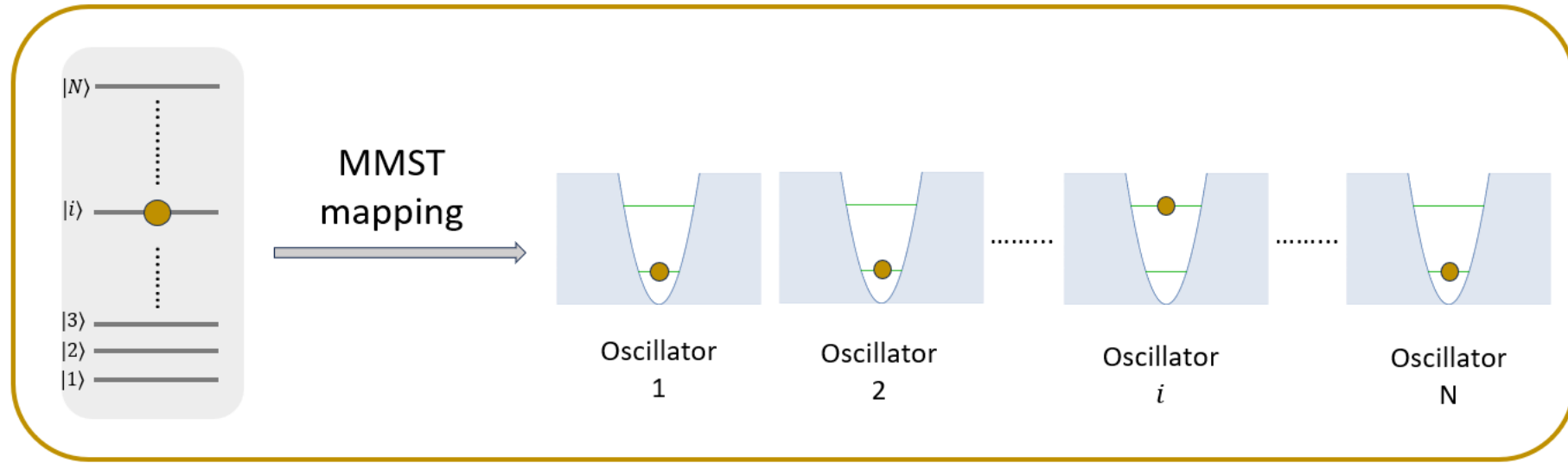
- $N \rightarrow \infty$
- Trotter approximation

$$= \int \mathcal{D}x e^{iS(x,x')/\hbar}$$

sum over paths



# MMST mapping



$$H_{sym}(\mathbf{X}, \mathbf{P}, \mathbf{x}, \mathbf{p}) = \frac{1}{2} \mathbf{P} \cdot \mathbf{M}^{-1} \cdot \mathbf{P} + \tilde{U}(\mathbf{X}) + \frac{1}{2} \left[ \mathbf{x} \cdot \tilde{\mathbf{V}}(\mathbf{X}) \cdot \mathbf{x} + \mathbf{p} \cdot \tilde{\mathbf{V}}(\mathbf{X}) \cdot \mathbf{p} \right],$$

$$\tilde{U}(\mathbf{X}) = U_0(\mathbf{X}) + \frac{N_e}{N+1} \text{Tr}[V(\mathbf{X})]$$

$$\tilde{\mathbf{V}}(\mathbf{X}) = \mathbf{V}(\mathbf{X}) - \frac{1}{N+1} \text{Tr}[V(\mathbf{X})] \mathbf{1}$$

# Initial Sampling

$$\hat{\rho} = |P_{Z_i}, Z_i\rangle\langle P_{Z_i}, Z_i| \otimes |\nu_i\rangle\langle \nu_i| \otimes \hat{\rho}_{\text{mol}} \otimes \hat{\rho}_{\text{metal}}.$$

Electronic dofs sampled using focused sampling.

$$\frac{1}{2}(x_k^2 + p_k^2 - \gamma) = n_k.$$

In spin mapping  $\gamma \rightarrow 0$  as  $N \rightarrow \infty$

-Bonella & Coker, Journal of Chemical Physics 2003, 118, 4370–4385

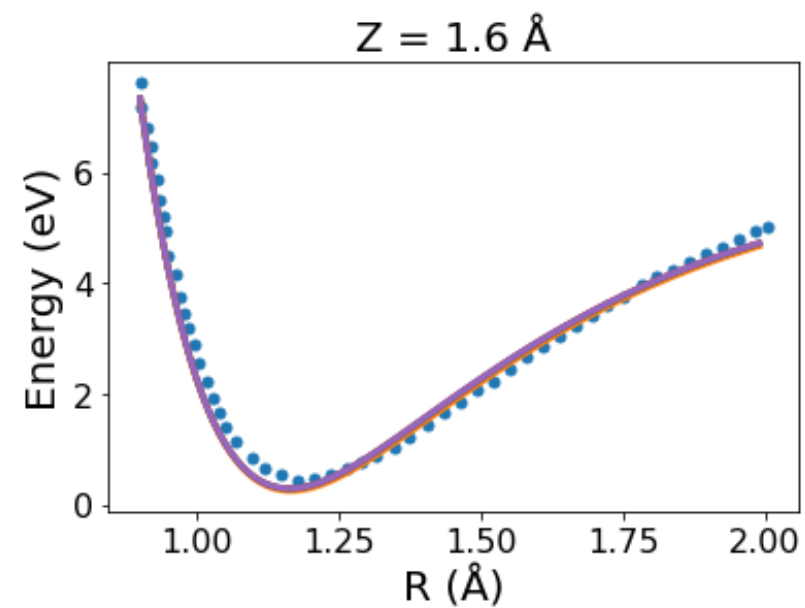
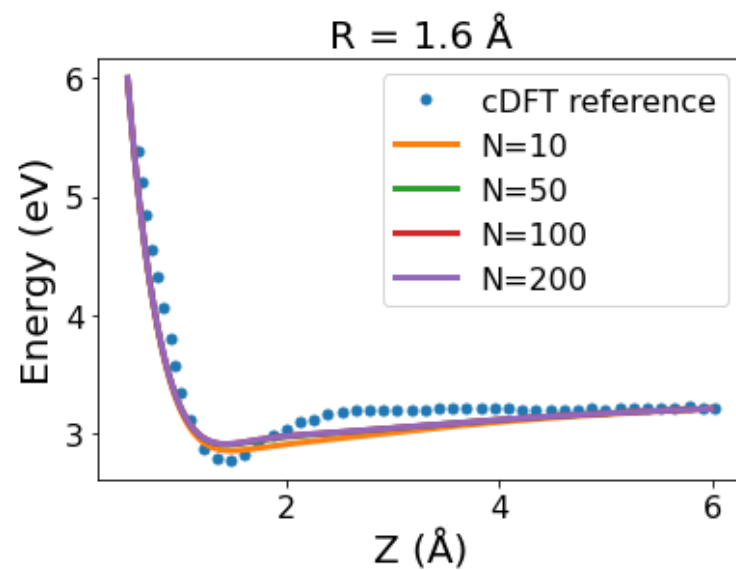
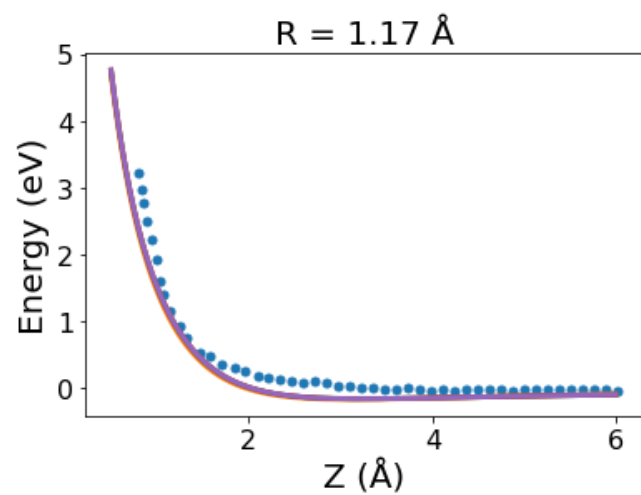
-Runeson & Richardson, The Journal of Chemical Physics 2019, 151, 044119.

# Replacing fermionic operators with bosonic ones

$$\begin{aligned}\langle \mathbf{n} | \hat{c}_j^\dagger(t_1) \hat{c}_k(t_2) | \mathbf{n} \rangle &= \sum_{j', k'} G_{j', j}^*(t_1) G_{k, k'}(t_2) \delta_{j', k'} \delta_{n'_k, 1} \\ &= \langle \mathbf{n} | \hat{b}_j^\dagger(t_1) \hat{b}_k(t_2) | \mathbf{n} \rangle,\end{aligned}\quad (20a)$$

$$\begin{aligned}\langle \mathbf{n} | \hat{c}_k(t_2) \hat{c}_j^\dagger(t_1) | \mathbf{n} \rangle &= \sum_{j', k'} G_{j', j}^*(t_1) G_{k, k'}(t_2) \delta_{j', k'} \delta_{n'_k, 0} \\ &= \langle \mathbf{n} | \hat{b}_k(t_2) \hat{b}_j^\dagger(t_1) | \mathbf{n} \rangle.\end{aligned}\quad (20b)$$

# GHM Refit



# GHM Refit

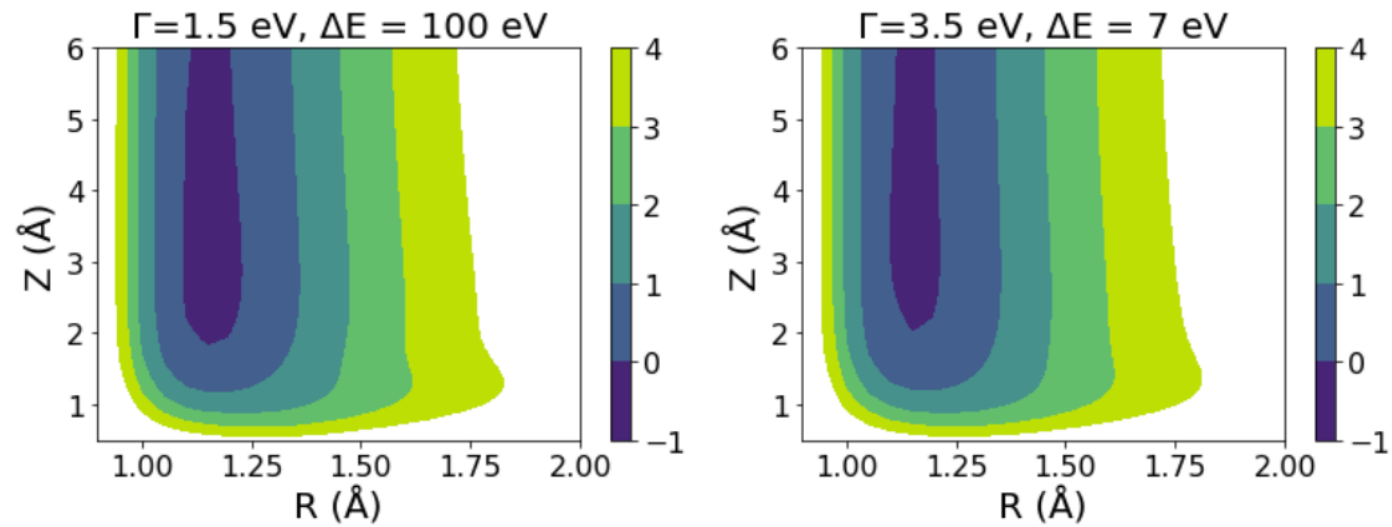
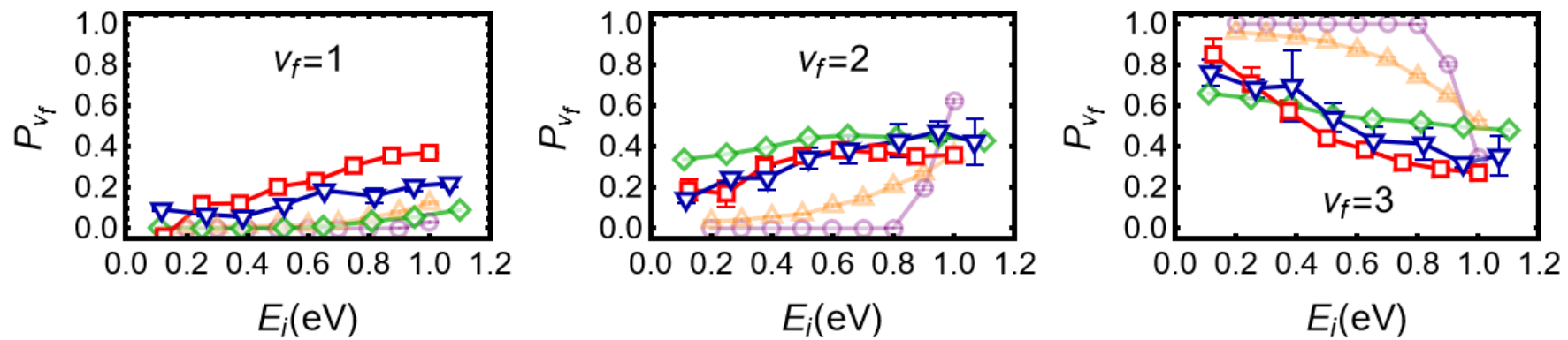
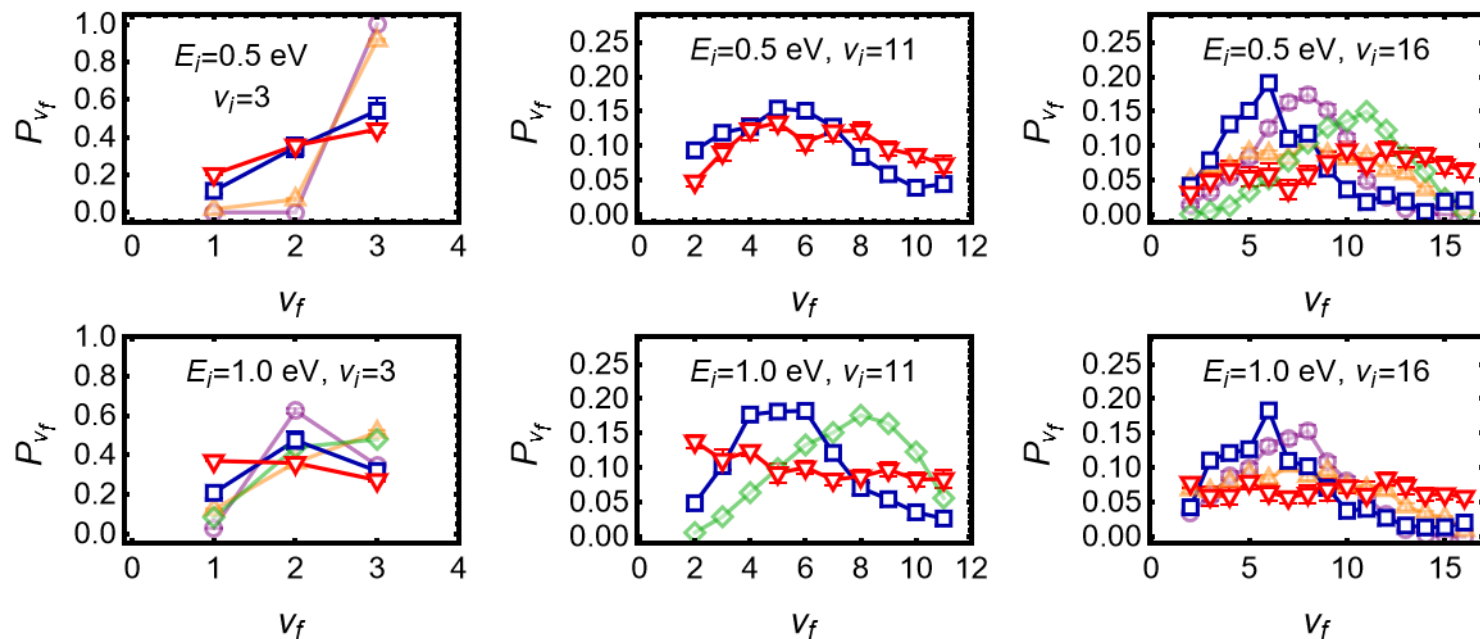


Figure S3: Contour plots of the adiabatic ground state energy for the model of Gardner et al. ( $\Gamma = 1.5\text{eV}, \Delta E = 100\text{eV}$ ) and our refit potential ( $\Gamma = 3.5\text{eV}, \Delta E = 7\text{eV}$ ).



— Exp — LSC — BCME — IESH — MDEF



— Exp. — LSC — BCME — IESH — MDEF